Available online at www.sciencedirect.com
ScienceDirect
Developmental Biology 301 (2007) 374–387
DEVELOPMENTAL BIOLOGY
www.elsevier.com/locate/ydbio

# *Pax6* controls the proliferation rate of neuroepithelial progenitors from the mouse optic vesicle

Robert-Hugues Duparc [a], Mohamed Abdouh [a], Jocelyn David [a], Mireille Lépine [a], Nicolas Tétreault [a], Gilbert Bernier [a,b,*]

[a] *Developmental Biology Laboratory, Maisonneuve-Rosemont Hospital, 5415 Boul. l'Assomption, Montreal, Canada H1T 2M4*
[b] *Department of Ophthalmology, University of Montreal, Montreal, Canada*

Received for publication 11 May 2006; revised 7 September 2006; accepted 4 November 2006
Available online 10 November 2006

**Abstract**

In vertebrates, a limited number of homeobox-containing transcription factors are expressed in the optic vesicle primordium and are required and sufficient for eye formation. At present, little is known about the distinct functions of these factors in optic vesicle growth and on the nature of the main neuroepithelial (NE) progenitor population present in this organ. We have characterized a multipotent cell population present in the mouse optic vesicle that shows extensive proliferation potential and which expresses NE progenitor and retinal markers *in vitro*. In *Pax6* mutant embryos, which form an optic vesicle, we found that the number of resident NE progenitors was greater than normal. *In vitro*, *Pax6*-null NE progenitors overproliferate and display reduced $p16^{Ink4a}$, $p19^{Arf}$, $p27^{kip1}$, $p57^{kip2}$, and $p21^{cip1}$ expression. Pax6 overexpression repressed cellular proliferation and secondary colonies formation, supporting the hypothesis that Pax6 acts cell-autonomously on NE progenitors cell cycle. Notably, these *in vitro* data correlated with aberrant numbers of mitosis observed in the optic vesicle of early stage *Pax6* mutants, with Pax6 association with the chromatin upstream of $p27^{kip1}$ promoter region, and with reduced expression levels of $p27^{kip1}$, $p57^{kip2}$, and $p21^{cip1}$ in the primitive forebrain of *Pax6* mutants. Taken together, our results suggest that, prior to retinal progenitor cell identity and neurogenesis, *Pax6* is required to regulate the proliferation rate of NE progenitors present in the mouse optic vesicle.


*Keywords:* Pax6; Optic vesicle; Retina; Homeobox transcription factor; Cell cycle; Neuroepithelial progenitors; Neurosphere assay; Lentivirus

## Introduction

Neuroepithelial (NE) progenitors represent the most primitive neural progenitors from which radial glial cells and adult neural stem cells of the central nervous system (CNS) are thought to derive (Gotz and Huttner, 2005; Huttner and Kosodo, 2005). NE progenitors form a stratified epithelium that lies within the ventricular wall of the developing neural tube (Huttner and Kosodo, 2005). The optic vesicle originates from the neural tube and is first detected around embryonic stage (e) 8.25 as a bilateral evagination of the anterior neural plate, named the optic sulcus (Oliver and Gruss, 1997; Marquardt, 2003). Around e9.5, the intimate contact between the optic vesicle and the eye surface ectoderm induces the transformation of the ectoderm into a lens placode, which is revealed by the proliferation and thickening of the ectoderm (Oliver and Gruss, 1997). In turn, the lens placode induces the evagination of the optic vesicle into an optic cup around e10.0. The optic cup ultimately gives rise to the neural retina and optic nerve fibers, while the surrounding neuroepithelium gives rise to the retinal pigment epithelium, optic stalk, and optic nerve myelinating sheet. These developmental processes are controlled by several morphogens and transcription factors which expression is finely regulated in time and space. One of these factors, Pax6, is a member of the paired-box and homeobox-containing gene family (PAX) of transcription factors and has been used as a prototype to study eye development in several model organisms (Gehring, 2002). In mice, *Pax6* is expressed starting at e8.0 in the eye surface ectoderm, and in the eye neural ectoderm, which gives rise to the optic vesicle (Walther and Gruss, 1991). Mice,

* Corresponding author. Maisonneuve-Rosemont Hospital, 5415 Boul. l'Assomption, Montreal, Canada H1T 2M4. Fax: +1 514 252 3569.
*E-mail address:* gbernier.hmr@ssss.gouv.qc.ca (G. Bernier).

0012-1606/$ - see front matter © 2006 Elsevier Inc. All rights reserved.
doi:10.1016/j.ydbio.2006.11.006

humans, and flies carrying homozygous mutations in *Pax6* are eyeless (Hogan et al., 1986; Glaser et al., 1994; Quiring et al., 1994; Grindley et al., 1995). Conversely, overexpression of *Pax6* in flies or frog embryos results in the formation of ectopic eyes, supporting the hypothesis that *Pax6* operates as a "master regulator of eye development in multi-cellular organisms" (Halder et al., 1995; Chow et al., 1999; Gehring, 2002; Gehring and Kazuho, 1999). Despite being anophthalmic at later stage of development, *Pax6*-null embryos form an optic vesicle that arrests in development prior to the optic cup stage (Hogan et al., 1986; Grindley et al., 1995). Tissue recombination and chimera aggregation experiments have revealed that *Pax6* is required cell autonomously for the specification of the lens ectoderm and formation of the lens placode (Fujiwara et al., 1994; Collinson et al., 2000). *Pax6* was also showed to control the proximo-distal patterning and homophilic and heterophilic cellular adhesion properties of the optic vesicle (Collinson et al., 2000). Notably, expression of *Rx*, *Lhx2*, *Otx2*, and *Six3*, all encoding transcription factors involved in early eye development, is apparently unaffected by the *Pax6* mutation, revealing that in mice, eye specification does occur in the absence of *Pax6* (Bernier et al., 2001). Conditional mutagenesis of *Pax6* in the retina around e10.5 also revealed that *Pax6* is required at the time of retinogenesis (Marquardt et al., 2001). In $Pax6^{\alpha\text{-}Cre}$ mutants, retinal progenitors underproliferate and give rise only to amacrine neurons, in part due to a failure to activate a specific set of pro-neural genes.

Herein we report on the characterization of multipotent and long-term proliferating NE progenitors located in the mouse optic vesicle. This cell population expresses NE and radial glia markers as well as early retinal patterning genes, including *Pax6*. We found that NE progenitors located in the optic vesicle of *Pax6* mutants are more abundant than normal and over-proliferate. Clonal cell dissociation assays revealed that Pax6 is expressed in colony-forming units. *In vitro*, NE progenitors lacking *Pax6* generate more symmetric cell divisions and have a reduced tendency to exit the cell cycle. *Pax6* overexpression repressed NE progenitors proliferation and secondary colonies formation in clonal assays, suggesting that *Pax6* act cell autonomously on NE progenitors proliferation. *Pax6* mutation results in reduced expression levels of several negative regulators of the cell cycle *in vitro* and *in vivo*, which may explain the observed overproliferation phenotype.

## Materials and methods

### *Animals*

Adult mice from the albino CD1 strain were purchased from Charles River (St-Constant, Qc., Canada). *Pax6* mutant mice are a gift from Peter Gruss (Max-Planck Institute, Goettingen). *Pax6* mutant mice and embryos were genotyped accordingly to St-Onge (St-Onge et al., 1997) and using LacZ staining in complementation. Embryo's stage was determined according to the time of vaginal plug.

### *Cell cultures*

Optic vesicles of e9.5 embryos were dissected out with tungsten needles in HBSS. Optic vesicles were directly triturated in HBSS using needles (20G-10×; 22G-5×) in order to obtain a suspension of single cells. After centrifugation, cells were placed in neural stem cell media: DMEM/F12 (Invitrogen) containing 0.25% glucose, B27 supplement, Heparin (2 μg/ml; SIGMA), Gentamycin (25 μg/ml; Invitrogen), and human recombinant FGF2 (10 ng/ml; SIGMA). Cells were cultured in 6 well plates (Sarstedt) for 3 to 10 days at 37°C in 5% $CO_2$ atmosphere. When applicable, BrdU (SIGMA) was added to the culture media at 10 μg/ml. For passage, single retinal spheres were dissociated with 0.25% trypsin (SIGMA)/culture media at 37°C for a period of time that was empirically established and that is proportional to spheres' size (1 min/13.5 μm of diameter). Trypsin was inhibited with 0.05% of trypsin inhibitor (SIGMA) in culture media. After trituration, the single cell suspension was harvested at 300 × *g* for 5 min and washed twice with HBSS. Cells were plated at 2000 cells/ml in neural stem cell media. Cell viability was evaluated using a hemacytometer and trypan blue exclusion staining.

### *Cell differentiation assays*

Retinal spheres were allowed to differentiate in chamber slides (Lab-tek) coated with poly-L-lysine (0.5 mg/ml; SIGMA) and laminin (10 ng/ml; SIGMA) in DMEM/F12 with 0.25% glucose, B27 supplement, Gentamycin (25 μg/ml) and 1% Fetal Bovine Serum (Invitrogen) at 37°C in 5% $CO_2$ atmosphere. After 10 days, cells were exposed to serum-free differentiation media containing BDNF (10 ng/ml) and NGF (50 ng/ml) for 5 days (Invitrogen).

### *Cell cycle analyses*

Propidium iodide staining was performed following the procedure described by Krishan (1975). $10^6$ cells were fixed overnight in 75% ethanol and incubated for 1 h on ice with Krishan solution containing PI (50 μg/ml; Molecular Probes). Acquisition of nuclei preparation was performed employing a FACScan flow cytometer (Becton Dickinson) and Lysis II acquisition software with the electronic doublet-discrimination module (DDM) activated. 20,000 events were recovered for each sample. The percentage of cells in the cell cycle phases was evaluated using the ModFit LT 3.0 software.

### *Immunofluorescence (IF)*

Samples were fixed in 4% PFA/PBS for 1 h, washed in PBS, and equilibrated overnight at 4°C in 30% sucrose/PBS. Samples were then immersed in cryomatrix solution (Shandon, Pittsburgh) and snap frozen in liquid nitrogen. Cryosections were performed at 7 μm, air dried on slides for 10 min, and washed 3× with PBS prior to blocking. For cell culture experiments, cells were fixed in 4% PFA/PBS for 10 min and washed with PBS. For BrdU labeling experiments, retinal spheres were directly frozen in liquid nitrogen and post-fixed after sectioning using 100% ETOH for 10 min and 1% PFA/PBS for 1 h. Sections or cells were treated with DNase I/0.05% HCl for 30 min in order to reveal BrdU epitopes. Samples were blocked in 1% BSA (Vector laboratories)/0.1% Tween 20/PBS solution and incubated with the primary antibodies overnight at 4°C. After washes with PBS, samples were incubated with appropriate secondary antibodies for 1 h at RT. Antibodies: Six3 (G. Oliver, St. Jude Children's Research Hospital); Nestin (BD Transduction Laboratory); BrdU and syntaxin, clone HPC-1 (SIGMA); Blbp (N. Heintz, The Rockefeller University); 4D2 (R. Molday, UBC); β-galactosidase (CORTEX BIOCHEM); P-H3 (Upstate); Thy1.2 (Cedarlane); and Bmi1 (US Biological). All others were from CHEMICON. Specificity of all antibodies was tested on frozen sections from whole embryos and adult mouse eyes. Secondary antibodies were used as negative controls in all experiments. TUNEL assay was performed accordingly to manufacturer instructions (Roche).

### *Viruses*

*Pax6* cDNA (P. Gruss, Max-Planck Institute, Goettingen) was cloned into EF.V.CMV.GFP (L. Cheng, Johns Hopkins University) and transfected in 293T cells with helper vectors (F. Boudreau, Sherbrooke University) using Lipofectamine 2000 (Invitrogen). Viral supernatants were ultra-centrifuged and exposed to single cell suspensions O/N. Aggregates were dissociated to single cells and plated at 2000 cells/ml in NSC media for 1 week. GFP

positive retinal spheres were visualized using a fluorescence-mounted inverted microscope (LEICA).

### *RT-PCR*

All primers were designed to flank individual exons and tested by PCR in RT+ and RT− retinal extracts. Total RNA was isolated using TRIzol reagent (Invitrogen). Reverse transcription (RT) was performed using 2 μg of total RNA and the MML-V reverse transcriptase (Invitrogen). PCR amplification was performed using the HotStar TAQ polymerase (Invitrogen). Real-time PCR was performed using the Platinum SYBRGreen SuperMix (Invitrogen) and a real-time PCR apparatus (BioRad). All experiments were performed in triplicates. Primer sequences are available upon request.

### *Chromatin ImmunoPrecipitation (ChIP) analyses*

ChIP was performed using the ChIP Assay Kit (Upstate, NY) according to the manufacturer's instructions. Briefly, $10^6$ cells were sonicated to shear the chromatin into 0.5–1 kb fragments. Pax6 and acetylated histone4 (A-H4) proteins and their associated protein–DNA complexes were isolated by immunoprecipitation with rabbit anti-Pax6 (US Biological) and rabbit anti-A-H4 (Upstate, NY) antibodies. Samples were heated to reverse the protein–DNA crosslinks and the DNA recovered by phenol/chloroform/isoamyl alcohol extraction. These DNAs were used as template for PCR amplification of Pax6 binding sites in the $p27^{kip1}$ gene. After a denaturation step of 5 min at 95°C, PCR was performed for 33 cycles, with 15 s at 95°C, 20 s at 58°C, and 30 s at 72°C. PCR primers sequences are available upon request.

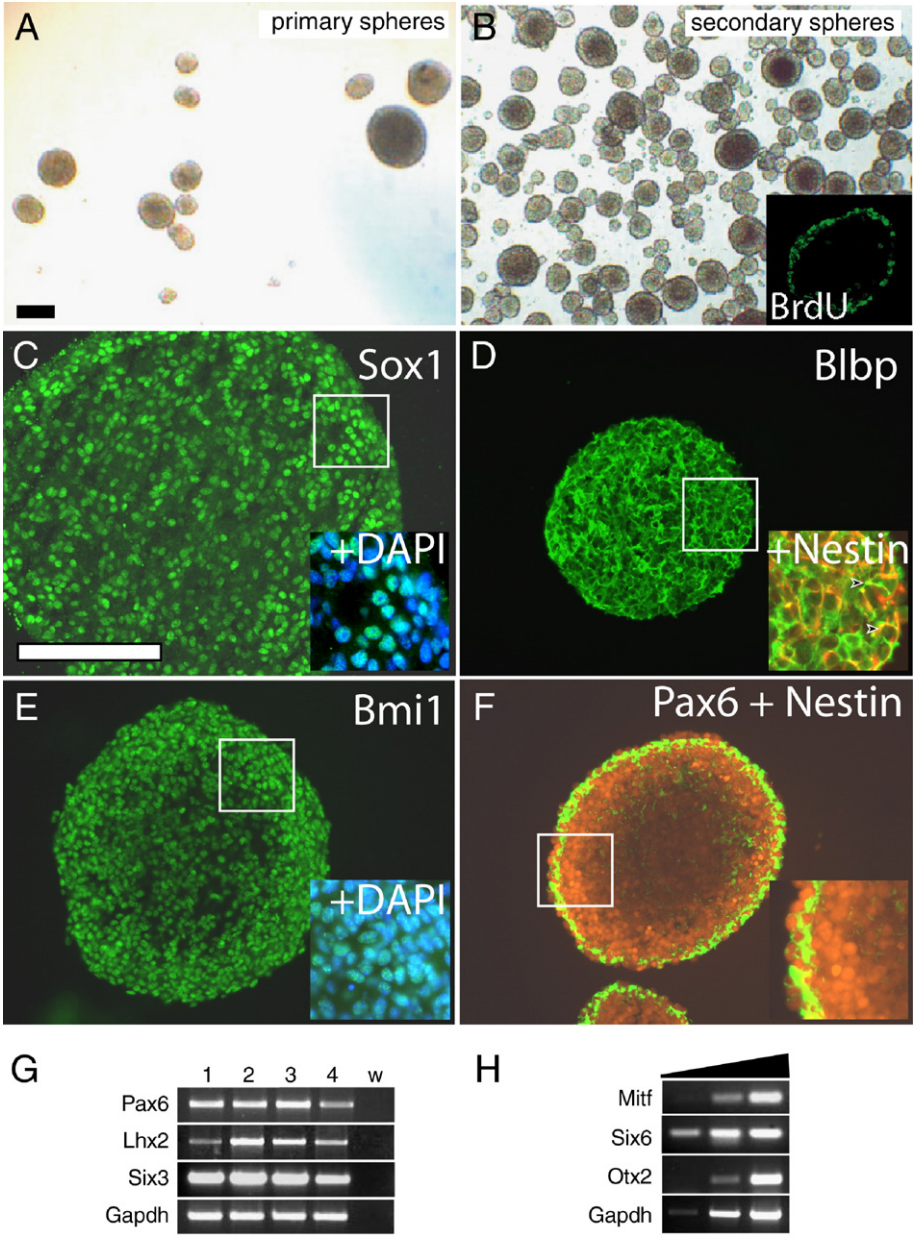


Fig. 1. NE progenitors from the mouse optic vesicle can generate floating sphere colonies. (A) Floating sphere colonies obtained from primary cultures of dissociated optic vesicles after 7 days. (B) Passage 1 of primary spheres resulted in the formation of multiple new secondary spheres showing BrdU incorporation (inset). (C–F) Retinal spheres express Sox1, Blbp, Nestin, Bmi1, and Pax6 as viewed by indirect IF on frozen sections. (G) Retinal spheres analyzed by RT-PCR (25 cycles) as single clones (1–4) or analyzed by semi-quantitative RT-PCR in bulk extracts (H). W: water control. Scale bars: (A and B) 500 μm, (C–F) 200 μm.

*Statistical analyses*

Data are presented as mean±standard deviation (error bars). Statistical analyses were performed using a one-tailed and unequal variance Student's *t* test. Values are representative of at least 3 experiments. Differences were considered statistically significant when $P$ was $<0.05$.

## Results

### *Isolation and characterization of NE progenitors from the mouse optic vesicle*

The optic vesicle neural ectoderm gives rise to all neural and glial cells present in the mature retina (Oliver and Gruss, 1997; Marquardt, 2003). To characterize the NE progenitors population present in this organ, we performed dissociated cultures of mouse optic vesicles at e9.5 in serum-free media containing the growth factors (GF) Fibroblast Growth Factor 2 (FGF2) at 10 ng/ml, Epidermal Growth Factor (EGF) at 20 ng/ml, both GFs or no GF (Tropepe et al., 1999). In the presence of FGF2 or FGF2+EGF, but not with EGF alone or no GF, a mean of 22 growing neurospheres (as confirmed by Bromodeoxy-Uridine (BrdU) incorporation) were obtained per embryo after 1 week in culture (Figs. 1A and B). Average number of cells per sphere was ~8000 after 1 week in culture. To test if these cells displayed self-renewal capability, single or pool of 10 spheres were dissociated to single cell suspensions (at day 10) at 2000 cells/ml and re-plated in the same media containing FGF2. On average, 70 novel growing neurospheres/10,000 cells (0.7%) were obtained after the first passage (Fig. 1B). Single spheres were assayed for their ability for long-term self-renewal by serial passages. We found that, after the second passage, FGF2 alone was not sufficient to promote neurospheres growth and that FGF2 and EGF were required. Under these conditions, neurospheres could be maintained for up to 8–9 passages, with a constant ratio of ~70 novel spheres/10,000 cells. This cumulated in the clonal expansion of retinal colonies number by a factor greater than $1\times10^9$.

Using DNA microarray hybridization and indirect immunofluorescence (IF), we found that isolated spheres from the optic vesicle expressed most NE progenitor (Sox1, Sox2, Nestin, CD133/prominin and Bmi1) and radial glia (Blbp) markers (Figs. 1C–E, Table 1 and data not shown) (Molofsky et al., 2003; Anthony et al., 2004; Ellis et al., 2004; Lee et al., 2005). Sox1, Blbp, and Bmi1 were expressed uniformly on retinal sphere sections, while Nestin expression was enriched at the sphere's periphery (Fig. 1). Sox1/Sox2 genes are expressed in the primitive neural ectoderm and by neural stem cells, and *SOX2* mutations are linked to anophthalmia in humans (Fantes et al., 2003; Ellis et al., 2004 and Table 1). Nestin is an intermediate filament expressed by neural progenitors, neural stem cells, and myoblasts (Zimmerman et al., 1994). CD133/prominin is a cell surface protein that localizes at the luminal surface of the neural ectoderm (Huttner and Kosodo, 2005). CD133/prominin has been used for the purification and enrichment of neural stem cells (Lee et al., 2005). Expression of CD133/prominin protein was found at the luminal surface of the optic vesicle neural ectoderm (RHD and GB, unpublished).

Table 1
Markers used to analyze retinal spheres

| Marker | Labeled cells in the developing CNS [a] | Expression in optic vesicles [b] | Expression in retinal spheres [c] |
|---|---|---|---|
| Sox1 | NE progenitors and stem cells | + | ++ |
| Sox2 | NE progenitors, stem cells, and retinal progenitors | + | ++ |
| Blbp | Radial glia | − | ++ |
| Bmi1 | NE progenitors and stem cells | + | ++ |
| Nestin | NE progenitors, progenitors, and stem cells | + | ++ |
| CD133 | NE progenitors and stem cells | + | + |
| Pax6 | NE progenitors, retinal and cortical progenitors, and radial glia | ++ | ++ |
| Six3 | Anterior neural plate and retinal progenitors | ++ | ++ |
| Lhx2 | Anterior neural plate, retinal, and cortical progenitors | ++ | ++ |
| Six6 | Retinal progenitors | + | + |
| Otx2 | Anterior neural plate, forebrain and midbrain neuroepithelium, RPE, and photoreceptor precursors | + | + |
| Mitf | Prospective and definitive RPE | + | + |

[a] Based on published expression patterns.
[b] Based on published expression patterns and unpublished data.
[c] As evaluated by DNA microarray hybridizations, indirect IF on sections, and RT-PCR analyses.

*Bmi1* has been show to be expressed by and to be required for the maintenance of CNS and neural crest stem cells proliferation after birth (Molofsky et al., 2003). Expression of Bmi1 protein was found throughout the optic vesicle neural ectoderm (RHD and GB, unpublished and Table 1). Blbp is a well-defined marker for radial glial cells, which serve as neural stem cells during CNS development (Anthony et al., 2004). We observed that Blbp expression levels were relatively low in the developing mouse retina at e12.5 and e15.5, in contrast to the developing brain (RHD and GB, unpublished and Anthony et al., 2004). Blbp expression was not detectable at e9.5 in the optic vesicle, suggesting that the robust Blbp expression we observed in retinal spheres may be induced by the culture conditions (Yoon et al., 2004 and Table 1). Taken together, these results revealed that, relative to the expression levels found in the optic vesicle, isolated spheres were enriched for the expression of radial glia and NE progenitor/stem cell-specific genes (Table 1).

In vertebrates, a limited number of homeobox-containing transcription factors define the retina field and are required for early eye formation (Hill et al., 1991; Oliver and Gruss, 1997; Oliver et al., 1995; Mathers et al., 1997; Porter et al., 1997; Jean et al., 1999). Furthermore, misexpression of *Pax6*, *Six3*, *Six6*, *Otx2*, and to a lesser extent *Rx* in frog or zebrafish embryos can induce ectopic retinal tissues (Mathers et al., 1997; Chow et al., 1999; Loosli et al., 1999; Zuber et al., 1999; Bernier et al., 2000). Using specific antibodies, we observed that all tested ($n=20$) neurospheres (as primary spheres or after passages 1–4) express the early retinal markers Pax6, Six3, and Lhx2 (Fig. 1F and data not shown). On sphere's sections, Pax6 localized to the cell's nucleus and was found to be most abundant at the sphere

periphery, where BrdU$^{+}$ and Nestin$^{high}$ cells were located (Fig. 1F). Expression of Pax6, Lhx2, Six3, Mitf, Six6, and Otx2 transcripts was also confirmed by RT-PCR on single spheres (Fig. 1G) or bulk extracts (Fig. 1H) (Table1). Thus, isolated spheres also expressed several early retinal-patterning genes, including Pax6.

*Retinal spheres are multipotent*

Tissue-specific progenitor/stem cells are characterized by their capacity to generate cell progenies with multiple differentiations potential (multipotent) (Temple, 2001). This differentiation potential is normally restricted to cell types found in the tissue of origin. In the retina, retinal progenitors are able to generate all six main neuronal cell types (ganglion, horizontal, amacrine, and bipolar neurons as well as cone and rod photoreceptors) and a single glial cell type (Müller glial cells) (Turner and Cepko, 1987; Turner et al., 1990). To test for this capacity, single sphere or pools of 10 retinal spheres (from passage 1, 2, 3, or 4) were plated on poly-L-lysine/laminin substrate in the presence of 1% FBS for 10 days and then switched to serum-free media containing the neurotrophic factors NGF and BDNF for 5 additional days. Using specific antibodies, we observed that retinal spheres could generate blue and red/green cone photoreceptors (~5–10%) (Figs. 2A and B), rod photoreceptor cells (~0.01%) (Fig. 2C), complex networks of amacrine neurons (~5%) (Fig. 2E), as well as Müller glial cells (~5%) (Fig. 2F). Recoverin$^{+}$ cells were also abundant (data not shown). Recoverin is expressed by photoreceptors and a subset of bipolar neurons. Horizontal cells (~0.1%) clearly positive with the 2H3 antibody, and PKCα positive neurons (thus possibly corresponding to bipolar neurons) were also observed (data not shown). However, ganglion cells were not detected under these culture conditions using a Brn3b antibody. Since ganglion cells do not survive well in culture, it is possible that most newly produced ganglion cells die by the time of our analyses (i.e. at day 15) (Huang et al., 2003). In addition, the Brn3b antibody we used was not very robust, even on whole eye

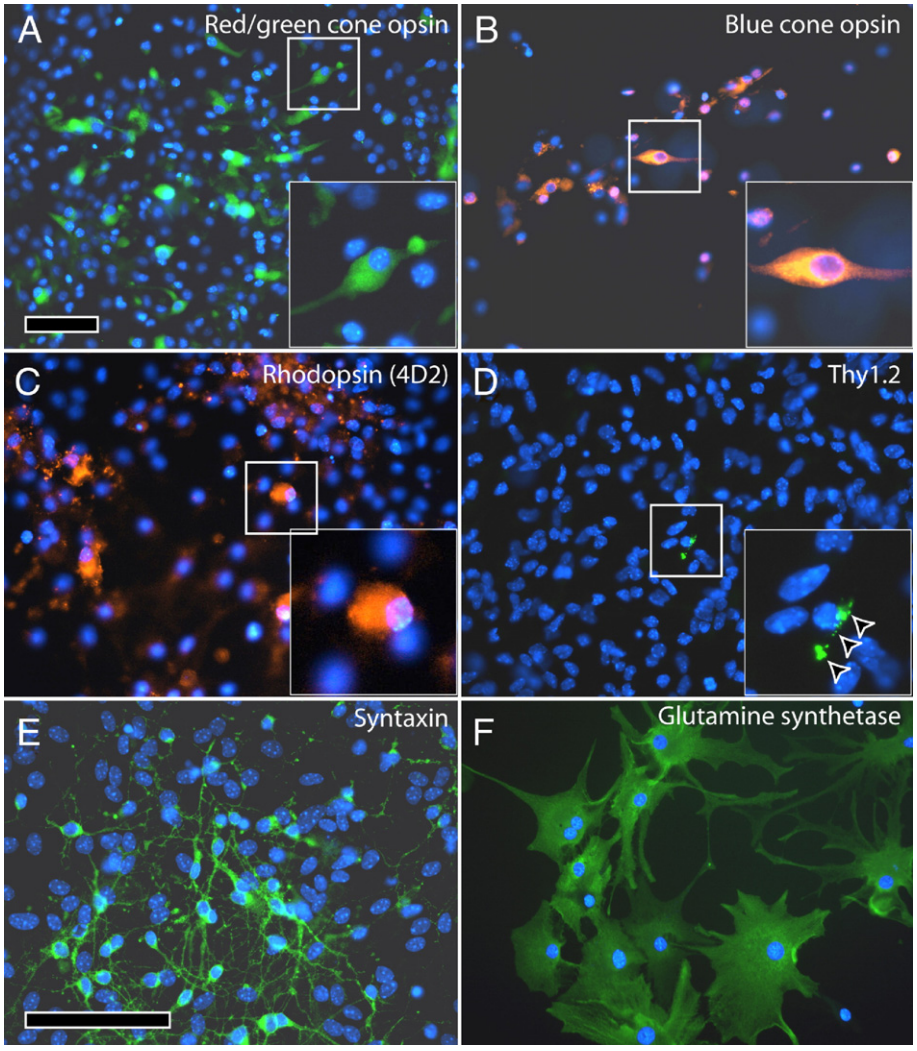


Fig. 2. Retinal spheres from the optic vesicle are multipotent. (A–F) Differentiated cells express markers for nearly all mature retinal cell types: (A) red/green cone photoreceptors; (B) blue cone photoreceptors; (C) rod photoreceptors; (D) ganglion cells; (E) amacrine neurons; (F) Müller glial cells. Scale bars: (A–D) 100 μm, (E and F) 100 μm.

sections. Single retinal spheres were induced to differentiate for only 6 days in the presence of 10 mM LiCl. LiCl is able to improve ganglion cells survival in culture (Huang et al., 2003). Day 6 was chosen for the analysis considering that TuJ1$^{+}$ immature neurons are first observed at day 3 of differentiation (data not shown). We used the Thy1.2 antibody, which recognizes a cell surface antigen expressed by nearly all ganglion cells, and Thy1.2$^{+}$ cells were observed at a rare frequency (Fig. 2D). We also observed the presence of mature oligodendrocytes (~0.1%) expressing the myelin basic protein, astrocytes (GFAP$^{+}$), immature (TuJ1$^{+}$), and mature (MAP2$^{+}$) neurons (data not shown). Notably, all single spheres tested ($n$=20) at passage 1–4 were capable to generate amacrine neurons, cone photoreceptors, and Müller glial cells, showing their multipotent nature in a clonal assay (RHD and GB, in preparation). Taken together, our data revealed that isolated retinal spheres were multipotent but more likely to produce cone photoreceptors, amacrine neurons, and Müller glial cells.

### *Pax6 is not required for the generation of NE progenitor colonies*

Despite being anophthalmic at a later stage of development, *Pax6*-null embryos develop an optic vesicle at e9.5. Notably, optic vesicles of *Pax6* mutants are broader than normal and failed to constrict proximally (Grindley et al., 1995). The presence of an optic vesicle allowed us to test if *Pax6* was required for the generation of NE progenitor colonies. Optic vesicles from wild type (WT) and *Pax6*$^{LacZ/LacZ}$ littermate embryos were dissected and cultured as described above in a neurosphere assay. In the absence of *Pax6*, retinal spheres did form. Notably, the mean number of retinal spheres obtained from *Pax6*$^{LacZ/LacZ}$ embryos was significantly higher than from WT embryos (27 versus 22) (WT; $n$=35 embryos and *Pax6*$^{-/-}$; $n$=37 embryos) (Fig. 3A). *Pax6* may not be required for the generation of retinal spheres at first but may be required for their long-term proliferation. To test for this possibility, single spheres from both genotypes were dissociated repeatedly in serial passages (for 7 generations). Both WT and *Pax6* mutant cells could be maintained equally under these conditions. Upon serial passage however, we found that newly generated retinal spheres were consistently more abundant in the *Pax6* mutant background than in WT. However, because *Pax6*-null spheres were also larger than WT (Fig. 4), normalization over the total number of cells per sphere was also performed. This resulted in a modest but significant difference between both genotypes, showing that the absolute number of colony-forming units is increased in the absence of *Pax6* (Fig. 3B).

*Pax6* may be expressed in most cells of the optic vesicle neural ectoderm and in most progenitors present in a retinal

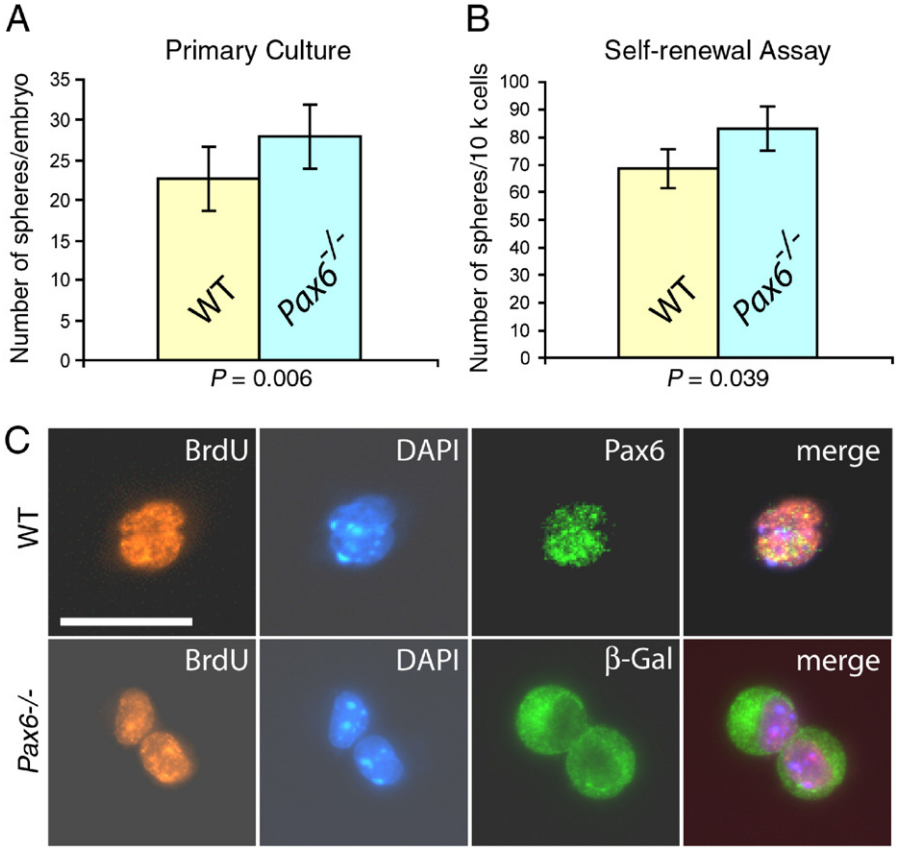


Fig. 3. *Pax6* mutation increases NE progenitors number. (A) Neurosphere assay on optic vesicles from WT ($n$=35) and *Pax6*$^{-/-}$ ($n$=37) embryos (mean±SD). (B) Secondary retinal spheres are more abundant when *Pax6* is mutated, as determined using clonal dissociation assays (mean±SD). WT ($n$=11) and *Pax6*$^{-/-}$ ($n$=12). (C) Dividing clone of cells was analyzed 48 h post-dissociation using antibodies against BrdU, Pax6, and β-galactosidase. Scale bar: 32 μm.

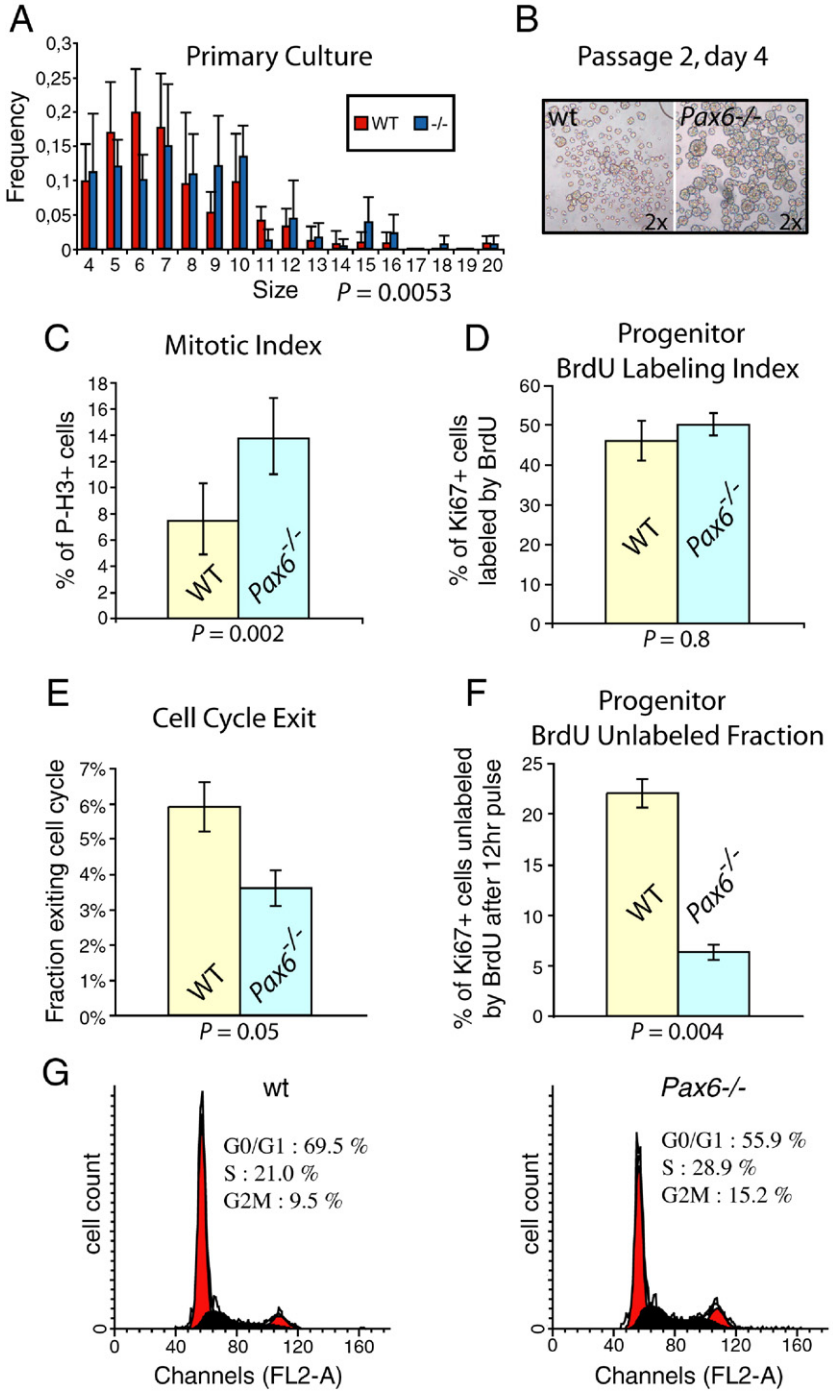


Fig. 4. *Pax6*-null retinal spheres overproliferate. (A) Size distribution of WT (number of cultures = 14) and $Pax6^{-/-}$ (number of cultures = 14) primary retinal spheres after 7 days in culture (mean ± SD). (B) Phase contrast observation. (C) Mitotic index (mean ± SD). (D) Progenitors BrdU labeling index (mean ± SD). (E) Cell cycle exit (mean ± SD). (F) Progenitors BrdU unlabeled fraction after 12 h of BrdU pulse (mean ± SD). (G) Cell cycle analysis of WT and $Pax6^{-/-}$ secondary retinal spheres dissociated to single cells and labeled with propridium iodide at day 4 of culture.

sphere, but it may be not expressed in colony-forming cells. To discriminate between these possibilities, WT and $Pax6^{LacZ/LacZ}$ primary retinal spheres were dissociated to single cells. Cells were plated at 1000 cells/ml in serum-free media containing FGF2 in bacterial culture dishes in the presence of the base analogue BrdU. Under these conditions, only colony-forming cells survived and proliferated (first cell division at 48 h, as empirically determined). At 48 h, cells were washed and allowed to adhere to poly-L-lysine glass slides for 6 h and then processed for indirect IF using antibodies against BrdU and Pax6 (WT cells) or β-galactosidase ($Pax6^{LacZ/LacZ}$ cells). Alternatively, cells were directly deposited onto charged glass slides and visualized. Clones of 2 cells, both positive for BrdU, were then analyzed. In all cases, BrdU positive clones were also

found positive for either Pax6 (20/20 in WT) or LacZ (20/20 in *Pax6*$^{LacZ/LacZ}$) (Fig. 3C). Taken together, these results revealed that *Pax6* mutation increases the frequency of symmetric proliferative cell divisions (Huttner and Kosodo, 2005) and that Pax6 is expressed in colony-forming units.

### *Pax6 controls NE progenitors proliferation*

*Pax6*-null retinal spheres were found to be larger than WT spheres in primary cultures and upon serial passage (Figs. 4A and B). This phenotype could result from a larger proportion of dividing progenitors, reduced cell cycle exit, reduced cell death or shorter cell cycle.

To evaluate the overall proliferation rate between the two cell populations, retinal spheres at day 7 of culture were labeled with an anti-P-H3 antibody, which identifies mitotic cells (Lien et al., 2006). Analyses were performed at this time point because retinal spheres were large enough to be handled for sectioning and IF. These analyses revealed about twice as many P-H3 positive cells in *Pax6*-null compared to WT retinal spheres (Fig. 4C). Retinal spheres from WT and *Pax6*$^{LacZ/LacZ}$ samples were analyzed for cell death using the TUNEL assay. No differences were observed between both genotypes (data not shown). To evaluate the relative cell cycle length, spheres from both genotypes were pulsed with BrdU for 60 min and analyzed on sections with antibodies against BrdU and Ki67 (Chenn and Walsh, 2002; Klezovitch et al., 2004). The Ki67 antigen is expressed at all phases of the cell cycle, but not in G0, and is used as a marker for progenitors (Scholzen and Gerdes, 2000; Endl et al., 2001). Using this approach, it is possible to estimate the relative cell cycle length of progenitors, considering that the length of the S phase is relatively constant in mammalian cells (Chenn and Walsh, 2002; Kee et al., 2002; Lien et al., 2006). We found that the proportion of Ki67$^{+}$BrdU$^{+}$ cells over the total number of Ki67$^{+}$ cells was comparable between both genotypes, suggesting that *Pax6* mutation does not grossly affect the length of the cell cycle (Fig. 4D). In order to evaluate the proportion of progenitors that exit the cell cycle or differentiate, retinal spheres were pulsed with BrdU for 12 h and the proportion of BrdU$^{+}$Ki67$^{-}$ cells over the total number of BrdU$^{+}$ cells was calculated. In this time-lapse, ~38% less *Pax6*-null cells were found to have exit the cell cycle when compared to WT, indicating that *Pax6*$^{-/-}$ NE progenitors are less likely to generate asymmetric cell divisions and withdraw from the cell cycle (Fig. 4E). In the same experimental setting, we also calculated the number of Ki67$^{+}$ cells that had not incorporated BrdU during a 12 h BrdU pulse over the total Ki67$^{+}$ cell population (Ki67$^{+}$BrdU$^{-}$/total Ki67$^{+}$). This in principle should estimate the proportion of progenitors that have not initiated S phase in a 12 h time-lapse. Notably, while about 22% of all WT progenitors had still not initiated S phase in this time-lapse, only 6% of all *Pax6*$^{-/-}$NE progenitors remained unlabeled by BrdU (Fig. 4F). This suggests that *Pax6* mutation increases the probability of progenitors to transit from the G1 phase to the S phase of the cell cycle. We compared the DNA content of WT and *Pax6*$^{LacZ/LacZ}$ retinal spheres by Fluorescence Activated Cell Sorting (FACS) at day 4 after passage, at a time when close to 95% of the cells present in these

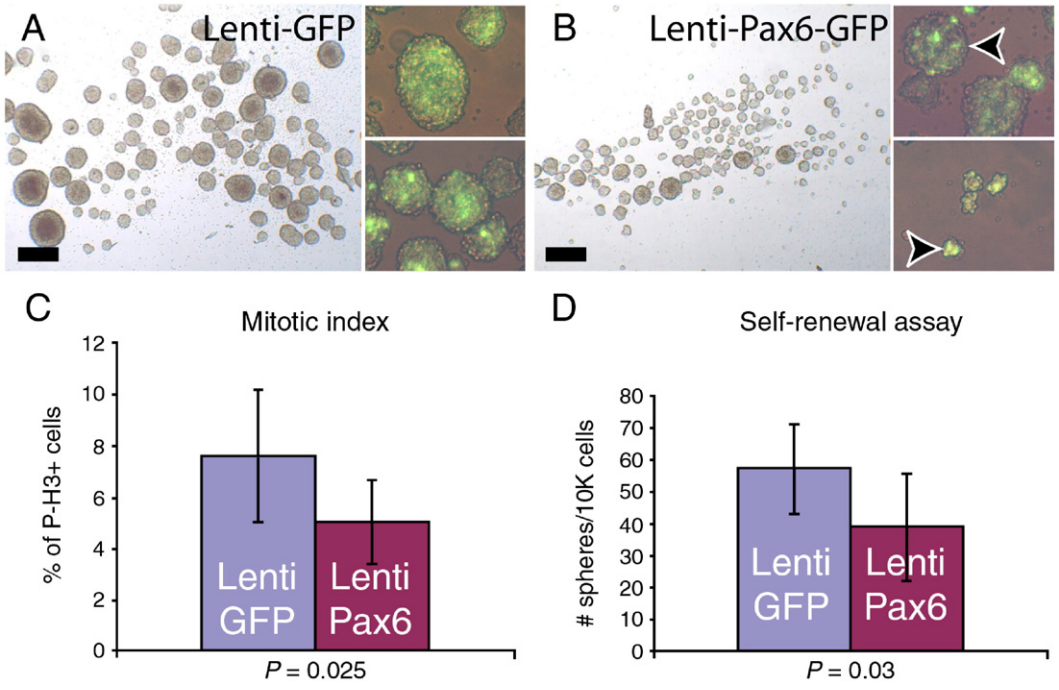


Fig. 5. *Pax6* overexpression represses retinal colony proliferation and secondary sphere formation. (A and B) WT retinal spheres infected with either Lenti-GFP or Lenti-Pax6-GFP viruses as observed in phase contrast 5 days post-infection. Lenti-GFP infected retinal spheres show relatively uniform fluorescence distribution (A, inset), while Lenti-Pax6-GFP infected retinal spheres (B, inset) show a fluorescence distribution that is in general variegated (arrowheads). (C and D) GFP and *Pax6/GFP* infected retinal spheres were analyzed for proliferation (mitotic index) or secondary sphere formation (self-renewal assay) at day 9 post-infection (mean ± SD). Scale bars: (A and B) 500 μm. Insets in panels A and B are at the same magnification.

small neurospheres are Ki67$^{+}$ (data not shown). In the absence of *Pax6*, 55.9% of all cells were in G0/G1 (compared to 69.5% in WT), 28.9% were in S phase (compared to 21% in WT), and 15.2% were in G2/M (compared to 9.5% in WT) (Fig. 4G). Taken together, these results suggest that *Pax6*$^{-/-}$ NE progenitors proliferate more because they have a greater tendency to transit from the G1 to the S phase of the cell cycle and a lesser tendency to generate asymmetric cell divisions and withdraw from the cell cycle.

To test whether *Pax6* could directly repress cell proliferation and colony formation, we overexpressed *Pax6* in WT retinal spheres (dissociated to single cells) using a lentivirus carrying *Pax6* and *GFP* (Yu et al., 2003). Viral infections were first performed at high cellular density (250,000 cells/ml), resulting in the formation of large adherent aggregates. Following re-dissociation and plating at low cell density in serum-free media, *Pax6*-transduced cells generated retinal spheres that were smaller than control-virus-infected spheres (Figs. 5A and B). Control-virus-infected spheres of large and medium size generally expressed GFP in most cells (Fig. 5A). In contrast, *Pax6*-virus-infected spheres of medium size generally expressed GFP in a variegated fashion while spheres expressing Pax6/GFP in most cells were very small, suggesting that overexpression of *Pax6* may force cells to withdraw from the cell cycle (Fig. 5B). Control- and *Pax6*-virus-infected retinal spheres expressing GFP were analyzed for P-H3 expression and

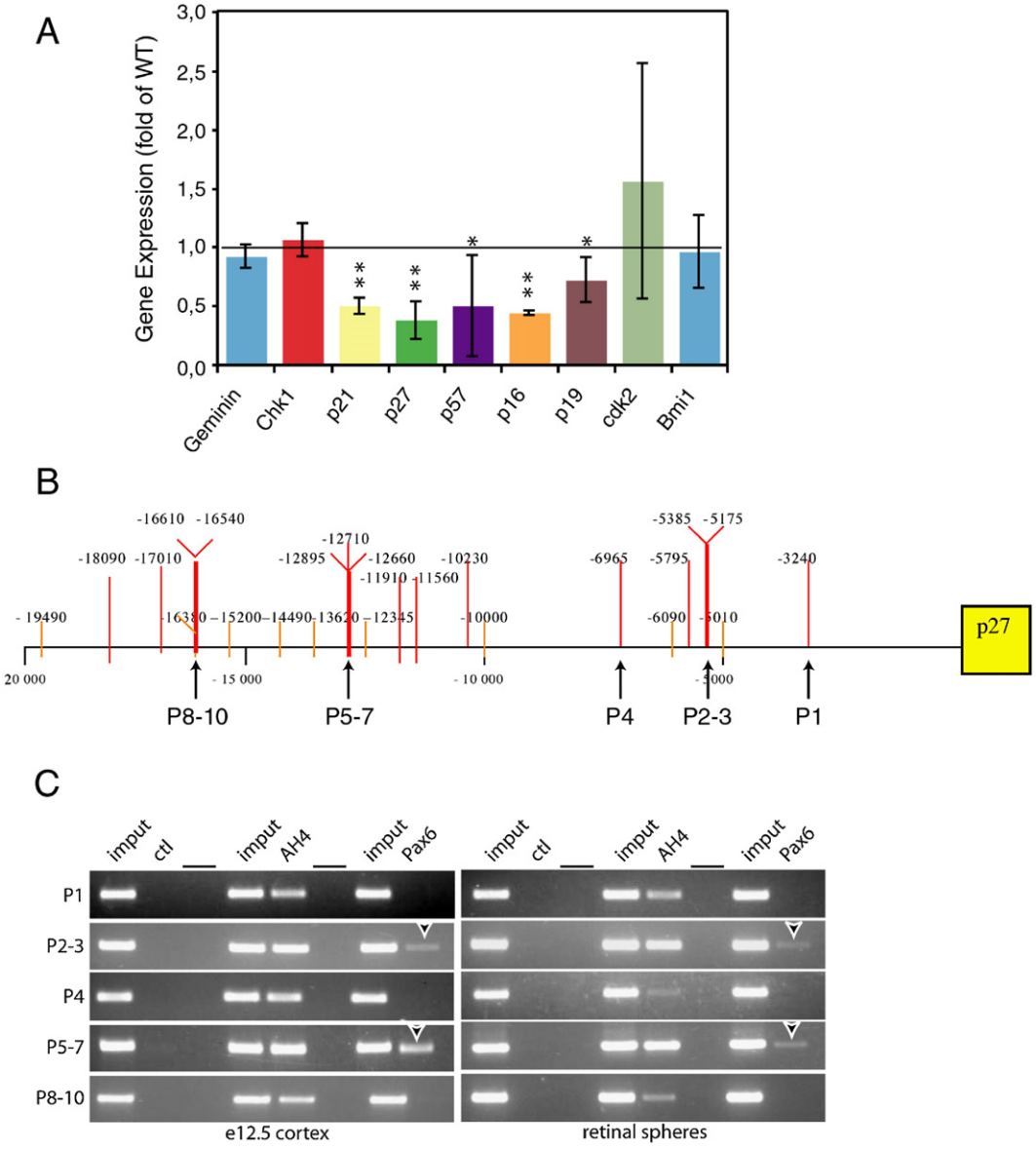


Fig. 6. Cell cycle regulatory genes are downregulated in *Pax6*-null retinal spheres. (A) Analysis of cell cycle regulator genes expression levels in *Pax6*-null retinal spheres using real-time PCR (mean±SD; values are normalized to *hprt* transcript). *$P<0.05$; **$P<0.001$. (B) Schematic representation of the genomic DNA sequence upstream of *p27 kip1* promoter region. The relative position of all putative Pax6 binding sites is indicated. "P" represents tested fragments in ChIP assays. (C) ChIP results on the genomic DNA sequences located upstream of *p27 kip1* promoter region using Pax6 and A-H4 antibodies. The no-antibody control (ctl) did not yield PCR bands for all tested primers. The input (2% of initial DNA) represents the chromosomal DNA that was not subjected to immunoprecipitation.

TUNEL labeling on sections. These results revealed a 40% reduction in mitotic figures upon *Pax6* transduction but no effect on cell death (Fig. 5C, and data not show). Virus-infected retinal spheres were also analyzed for the expression of Ki67. The total number of $Ki67^{+}$ cells over the total number of $DAPI^{+}$ cells was comparable between both groups (24%±6% for *GFP*-virus compared to 22%±11% for *Pax6*-virus), suggesting that Pax6 overexpressing cells do not exit the cell cycle but rather arrest in G1. However, because small spheres expressing *Pax6*-virus could not be analyzed on sections, we cannot rule out that, when expressed at higher levels, Pax6 can also force the cells to exit the cell cycle. *Pax6*- and control-virus-infected GFP positive spheres of comparable size were also dissociated to single cells and plated at low cell density in serum-free media to test for secondary colonies formation. When calculated in absolute number or relative to the total number of cells/sphere, the number of secondary spheres generated in *Pax6*-virus-infected spheres was significantly lower than those found in control-virus-infected spheres (Fig. 5D). Taken together, these analyses indicate that *Pax6*-overexpressing NE progenitors proliferate less and generate fewer symmetrical cell divisions.

### *Reduced $p16^{Ink4a}$, $p19^{Arf}$, $p27^{kip1}$, $p57^{kip2}$, and $p21^{cip1}$ expression in Pax6-null colonies*

To address the possible molecular basis of the overproliferation phenotype we observed, WT and *Pax6* mutant retinal spheres were analyzed for the expression of cell cycle regulator genes previously implicated in the control of retinal progenitor cells (i.e. Geminin, $p27^{Kip1}$, and $p57^{Kip2}$) and neural stem cells (i.e. Bmi1, $p16^{Ink4a}$, $p19^{Arf}$, and $p21^{Cip1}$) proliferation (Dyer and Cepko, 2001; Molofsky et al., 2003; Del Bene et al., 2004; Kippin et al., 2005). CDK2 and Chk1 were also tested and used as controls for the general cell cycle machinery. In *Pax6* mutant retinal spheres, expression levels of $p16^{Ink4a}$, $p19^{Arf}$, $p27^{kip1}$, $p57^{kip2}$, and $p21^{cip1}$ were all reduced by 40–60%, while expression levels of other genes were comparable to WT (Fig. 6A). Notably, $p21^{cip1}$-null neural stem cells overproliferate

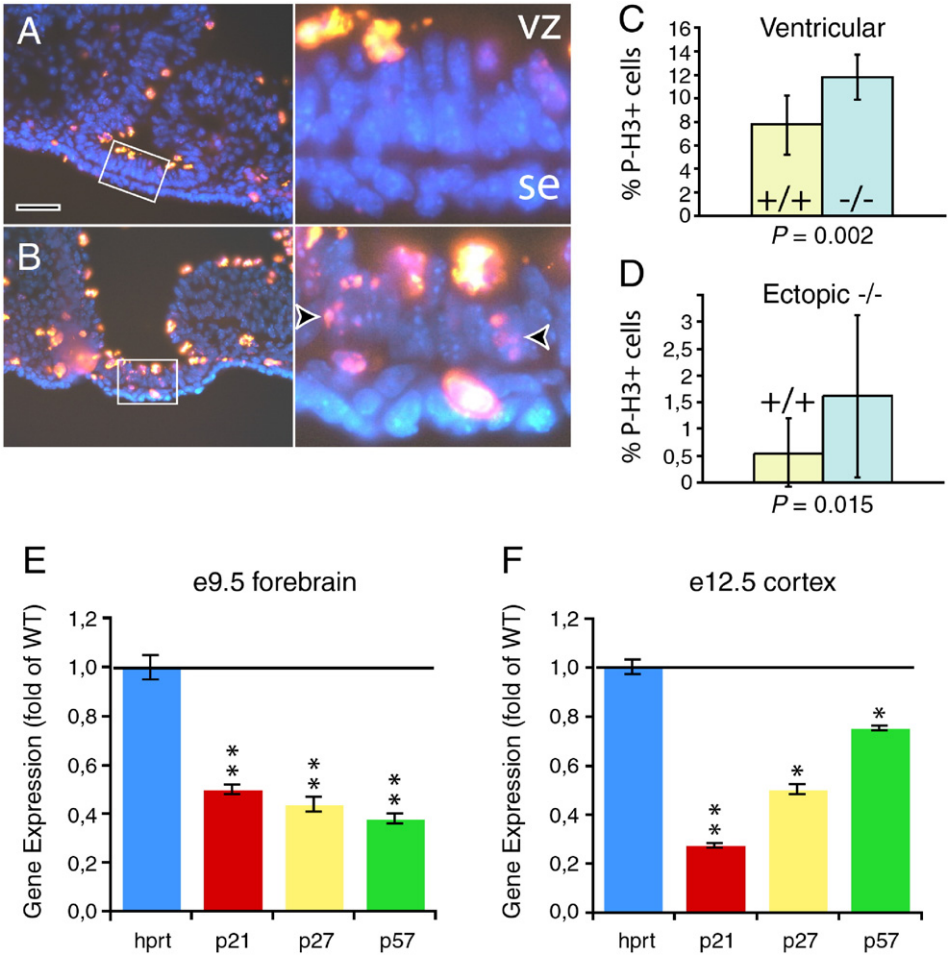


Fig. 7. NE progenitors in the optic vesicle of early *Pax6* mutant embryos overproliferate. (A and B) Indirect IF on optic vesicle sections from WT and *Pax6*-null littermate embryos at the 18 somites stage using an anti-P-H3 antibody. Transverse sections are showed. (C and D) Quantification analyses of cellular proliferation in the ventricular zone (vz) or between the eye surface ectoderm (se) and the ventricular zone (arrowheads in the inset) (mean±SD). (E and F) Analysis of $p21^{cip1}$, $p27^{kip1}$, and $p57^{kip2}$ expression levels in *Pax6* mutants using real-time PCR (mean±SD; values are normalized to *hprt* transcript). *$P<0.05$; **$P<0.001$. Littermate embryos (2 WT and 2 $Pax6^{-/-}$) were analyzed at 22 somites (e9.5 forebrain) or at e12.5. Scale bar: (A and B) 100 μm.

while $p27^{kip1}$ and $p57^{kip2}$ have been implicated in cell cycle control of retinal progenitors and in self-renewal of hematopoietic stem cells (Dyer and Cepko, 2001; Hock et al., 2004; Kippin et al., 2005). *Bmi1* was shown to repress $p16^{Ink4a}$ and $p19^{Arf}$ in neural stem cells, but *Bmi1* expression was unchanged in *Pax6*-null retinal colonies.

To test for a possible direct regulation by Pax6, we analyzed the non-coding genomic DNA sequences located upstream of $p27^{kip1}$, $p57^{kip2}$, and $p21^{cip1}$ transcription start sites for the presence of putative Pax6-binding sites. Several sites were found in all 3 genes, but these were especially abundant upstream of $p27^{kip1}$ promoter region (Fig. 6B). Ten putative binding sites were tested for direct association of Pax6 with the chromatin by ChIP using extracts from retinal spheres and e12.5 neocortex. Neocortex was used here because *Pax6* mutant cortical progenitors also overproliferate *in vivo* and *in vitro*, suggesting that Pax6 may control the cell cycle of NE progenitors from the optic vesicle and neocortex similarly (Gotz et al., 1998; Estivill-Torrus et al., 2002; Heins et al., 2002). As a positive control, we used an antibody against the acetylated form of Histone H4, which is normally associated with transcriptionally active chromatin. With both group of samples, we found a robust association of Pax6 with the chromatin fragments containing the P5–7 sites (located at positions −12,895, −12,710, and −12,660) and, to a lesser extent, the P2–3 sites (located at positions −5385 and −5175) (Fig. 6C). Taken together, these experiments revealed that *Pax6* is required for proper expression of $p16^{Ink4a}$, $p19^{Arf}$, $p27^{kip1}$, $p57^{kip2}$, and $p21^{cip1}$ in retinal colonies and that Pax6 can directly associate with the chromatin upstream of $p27^{kip1}$ promoter region.

### *Pax6 controls cellular proliferation in the optic vesicle neural ectoderm*

Because *Pax6*-null NE progenitors display an overproliferation phenotype *in vitro*, we investigated whether NE progenitors located in the optic vesicle of *Pax6* mutants displayed a comparable phenotype. For this, WT and *Pax6*-null littermates at the 18 somites stage were analyzed for cell death and proliferation. This developmental stage was chosen because it precedes the lens placode induction stage, which is defective in *Pax6* mutants. Using the TUNEL assay, we did not observe a significant difference in the cell death rate between WT and *Pax6* mutant optic vesicles (data not shown). However, while the overall number of DAPI positive nuclei per optic vesicle section was comparable for both genotypes at this stage of development, there was a significant difference in the number of mitotic figures in the ventricular zone, as revealed by labeling with an anti-P-H3 antibody, which marks cells that are in G2/M (Figs. 7A and B). In *Pax6* mutant optic vesicle, ~11–12% of progenitor cells were in mitosis compared to ~8% in WT (Fig. 7C). Furthermore, in *Pax6*-null samples, numerous low P-H3 positive cells were found between the eye surface ectoderm and the ventricular zone of the optic vesicle (1.5% in Pax6 mutants compared to 0.5% in WT) (Fig. 7D). To investigate whether the expression of cell cycle repressors was also affected *in vivo*, the forebrain of 22 somites stage WT and $Pax6^{-/-}$ embryos was dissected and transcripts expression levels analyzed by real-time PCR. Parallel experiments were also performed with RNA extracts isolated from the neocortex of WT and $Pax6^{-/-}$ embryos at e12.5. As shown in Fig. 7, expression levels of $p21^{cip1}$ $p27^{kip1}$, and $p57^{kip2}$ were all significantly reduced in the forebrain and neocortex of *Pax6* mutants. These results revealed that, at early stages of ocular and cortical development, *Pax6* is required to control the proliferation rate of NE progenitors and normal expression levels of $p21^{cip1}$ $p27^{kip1}$, and $p57^{kip2}$.

## Discussion

We have identified a cell population localized in the mouse optic vesicle that displays characteristics of immature retinal progenitor/stem cells, i.e. capable of long-term proliferation and with the potential to generate multiple retinal cell types. This cell population expresses NE progenitor, radial glia, and retinal identity markers. In cell dissociation assays, we demonstrated that the Pax6 protein is expressed in colony-forming cells. We showed that, in $Pax6^{LacZ/LacZ}$ mutants, this endogenous NE progenitor population is more abundant than normal. Importantly, the $Pax6^{LacZ/LacZ}$ mutants carry a deletion in the entire paired domain of *Pax6* and thus are identical to the classical *Small eye* (Sey18) and conditional $Pax6^{flox/flox;a\text{-}Cre}$-null mutants (St-Onge et al., 1997; Marquardt et al., 2001). *In vitro*, *Pax6*-null NE progenitors showed increase symmetrical cell divisions and proliferation. Conversely, *Pax6* viral transduction repressed colonies formation and proliferation. *In vivo*, NE progenitors located in the optic vesicle of early stage *Pax6* mutants also overproliferate. *In vitro* and *in vivo*, *Pax6* mutation resulted in downregulation of key regulator genes of cell cycle progression, and this correlated with Pax6 association with the chromatin upstream of $p27^{Kip1}$ promoter region.

### *Multipotent NE progenitors in the mouse optic vesicle*

NE progenitors having the capacity to generate floating retinal colonies *in vitro* at clonal cell density represent only a fraction of the entire progenitor cell population present in the optic vesicle. In our hands, an average of 11 floating spheres/optic vesicle were obtained. Once established, these colonies could be maintained for a maximum of 8–9 generations using the neurosphere assay on single clones. The proliferation and expansion potential of these retinal colonies were found to be comparable to that reported for fetal cortical progenitor/stem cells. Retinal colonies differentiation's potential and growth factor requirement changed during serial passages. Both FGF2 and EGF were required from passage 2, and this correlated with an increase in the number of glial cells produced upon induction of cell differentiation after passage 2 (data not shown). This is in accordance with previous work showing that the combined action of FGF2 and EGF promotes gliogenesis in cortical progenitors (Lillien and Raphael, 2000; Viti et al., 2003). The differentiation potential of retinal colonies to generate both amacrine neurons and cone photoreceptors remained nearly

unchanged up to at least passage 4, the latest differentiation assay we performed (data not shown). *Pax6*-null retinal spheres were also induced to differentiate to test their multiple differentiation's potential (data not shown). Surprisingly, they could differentiate into multiple retinal cells types, including amacrine neurons (RHD and GB, in preparation). Ongoing experiments are aimed to understand the underlying mechanism regulating this phenomenon.

Work performed in the mouse lend to the identification of at least two distinct progenitor cell populations in the developing retina, i.e. pigmented retinal "stem cells" from the ciliary body (which arise around e14.5) and retinal progenitors of the neural retina (Tropepe et al., 2000). Within the developing neural retina itself, evidences suggest the possibility that two distinct progenitor cell population may also exist, as determined by the expression of the cell surface antigen SSEA-1 (Koso et al., 2006). SSEA-1 is predominantly expressed by immature retinal progenitors located at the retinal ciliary margin but not by $Ki67^{+}$ progenitors located in the central retina and neither by mature progenitors found at early post-natal stages (Koso et al., 2006). One arising question regarding the present study is whether NE progenitors from the optic vesicle identified here have a lineal relationship with retinal progenitors, pigmented retinal "stem cells", or both. In principle, NE progenitors represent the most primitive neural progenitors and embryological studies indicate that both the neural retina and ciliary body originate from the optic vesicle (reviewed by Hyer, 2004). Thus, all progenitors found in the developing retina and ciliary body should originate from the optic vesicle. However, by using the neurosphere assay, we have imposed a stringent selection on the progenitor cell population present in the optic vesicle, and it is not known at the moment to which extent this specific cell population is comparable to other types of retinal progenitors found later in development. Further work using genetics analyses, cell surface antigens, and molecular markers will be required to answer this question.

### *Pax6 and the regulation of NE progenitors cell cycle in the optic vesicle*

We found that *Pax6*-null retinal colonies: (i) generate more symmetric proliferative division; (ii) have a decrease tendency to exit the cell cycle; (iii) underexpress the cell cycle repressors $p16^{Ink4a}$, $p19^{Arf}$, $p27^{ki1}$, $p57^{kip2}$, and $p21^{cip1}$, which are known to regulate the G1 to S phase transition of the cell cycle as well as cell cycle exit. Taken together, these results reveal that *Pax6* has an important role in the coordination of NE progenitors cell cycle and this conclusion is further supported by the abnormal number of mitosis we observed in the optic vesicle of 18 somites stage *Pax6* mutant embryos. In these embryos, we also observed a 3-fold increase in the number of "ectopic" $P\text{-}H3^{+}$ cells, suggesting either an abnormal cellular organization and/or aberrant cell cycle. Based on this, we propose that an appropriate interpretation of *Pax6* function in the context of normal optic vesicle development may be not the one of a cell cycle repressor *per see* but rather of a coordinator of the cell cycle kinetics.

One arising question is why conditional mutation of *Pax6* in retinal progenitors at e10.5 resulted in reduced cellular proliferation while *Pax6*-null NE progenitors overproliferate? One possible explanation is that *Pax6* function is context-dependent during retinal development. For example, the co-expression of other transcription factors may modulate distinct Pax6 transcriptional activities during optic vesicle and retinal development. Similarly, *Pax6* biological function may change as development proceeds because of modifications in the microenvironment or progenitors competence state. Alternatively, *Pax6* may modulate conflicting activities that are in an equilibrium state in normal conditions (i.e. proliferation versus differentiation). For example, *Mash1* is apparently upregulated in the optic vesicle of *Pax6* mutants at e9.5, despite being dependent on *Pax6* activity for its expression in the developing retina at e10.5 (Marquardt et al., 2001; Philips et al., 2005). A comparable paradox also exists in the telencephalon of *Pax6* mutants where cortical progenitors overproliferate at e12.5 but underproliferate at e15.5 (Estivill-Torrus et al., 2002). Finally, *Pax6* may also display both cell-autonomous and non-cell-autonomous activities, and non-cell-autonomous activities may arise at the time of neurogenesis, when *Pax6* is expressed in proliferating retinal progenitors and in ganglion cells and amacrine neurons.

In addition to cell cycle regulators we identified here, *Pax6* action on NE progenitors proliferation may be also mediated through regulation of molecules controlling cell–cell interactions (i.e. adherens junctions) and/or adhesion to the apical membrane (i.e. apical membrane junctions) (Klezovitch et al., 2004; Huttner and Kosodo, 2005; Lien et al., 2006). In *Pax6* mutants, the optic vesicle neuroepithelium is defective in autologous and heterologous cellular adhesion, suggesting an intrinsic defect in the expression of molecules involved in cellular adhesion (Collinson et al., 2000). This is important since recent findings have established that the mode of cell division of NE progenitors is in part determined through cellular interactions present at the apical membrane process (Huttner and Kosodo, 2005) and that inactivation of the adherens junction protein alphaE-catenin induces overproliferation of cortical progenitors (Lien et al., 2006). Recently, we found that *Pax6* was required for the expression of *Delta-catenin/neurojugin* in the optic vesicle, neocortex, and cerebellum of mice (Duparc et al., in press). Delta-catenin is a cytoskeletal protein that localizes at adherens junctions and which directly interacts with and regulate N-Cadherin in the CNS. Thus, the apical–basal polarity of NE cells is important to control the mode of cell division and this polarity may be altered in the CNS of *Pax6* mutants.

Importantly, studies on *Pax6* function in cerebral cortex argue in the same sense as our observations made in the optic vesicle (Gotz et al., 1998; Estivill-Torrus et al., 2002; Heins et al., 2002). BrdU labeling studies have revealed that cortical progenitors of $Pax6^{-/-}$ embryos at e12.5 proliferate more than WT progenitors *in vivo* (Estivill-Torrus et al., 2002). *In vitro*, cortical radial glial cells of $Pax6^{-/-}$ mutants develop into larger colonies than WT (Heins et al., 2002). Conversely, radial glial colonies overexpressing *Pax6* and placed under adherent cell

culture conditions were shown to produce smaller colonies containing almost exclusively neurons (Heins et al., 2002). Notably, Estivill-Torrus et al. have established that cortical progenitors lacking *Pax6* have a shorter cell cycle, including a marked reduction in the length of the S phase (Estivill-Torrus et al., 2002). This observation is singular since the length of the S phase is generally constant in mammalian cells (Kee et al., 2002). Thus, these results differ form our observations, where a significant reduction in cell cycle length was not observed. However, these differences could be explained by the different methodologies used (linear regression analyses compared to progenitor BrdU labeling index) and/or by the different systems analyzed (embryonic cortex versus retinal spheres). Notably, we observed that the proportion of progenitors having initiated the S phase over a 12 h time period was greater in *Pax6*-null retinal colonies, suggesting that the relative quiescence of NE progenitors in G1 may be affected by the *Pax6* mutation. Regardless of these differences, the overall conserved function of *Pax6* in regulating NE progenitors proliferation in both the optic vesicle and neocortex suggests a more general function for *Pax6* in controlling cellular proliferation. For example, *Pax6* overexpression was recently shown to induce neurogenesis and $P21^{CIP1}$ expression in human HeLa cells (Cartier et al., 2006). More surprisingly, low *PAX6* expression level is an unfavorable prognostic marker in glioblastoma, while *PAX6* overexpression antagonizes glioblastoma colony formation in soft-agar assays and brain tumor growth in xenotransplants (Zhou et al., 2003, 2005). These results may be explained by the capacity of *Pax6* to induce neurogenesis and repress cellular proliferation when overexpressed. At the opposite, loss of *PAX6* in glioblastoma may result in a more undifferentiated state together with an increase in cellular proliferation. Importantly, Pax6 function in neurogenesis and cellular proliferation can be uncoupled at the molecular level. While the canonical form of Pax6 contains both neurogenic and anti-proliferative activities within its paired domain, the Pax6(5a) isoform, which has a 14 amino-acid insertion within the N-terminal region of the paired domain, displays only anti-proliferative activities (Haubst et al., 2004). These results imply that distinct Pax6-target genes control neurogenesis and cellular proliferation (Haubst et al., 2004).

In conclusion, we have identified multipotent and long-term proliferating NE progenitors present in the mouse optic vesicle and revealed that *Pax6* is required to control their proliferation rate and mode of cell division, most likely through regulation of $p16^{Ink4a}$, $p19^{Arf}$, $p27^{kip1}$, $p57^{kip2}$, and $p21^{cip1}$ cell cycle regulators. Further work will be required to prospectively isolate this cell population, determine its potential lineal relationship with retinal progenitors and pigmented retinal "stem cells", and dissect the molecular network controlling its development, proliferation, and multi-differentiation potential.

## Acknowledgments

Thanks to Mark Lesk for critical reading of the manuscript. This work was supported in part by a grant from the Natural Science and Engineering Research Council of Canada and Foundation Fighting Blindness of Canada. M.L. has a Pre-doctoral Scholarship from the FRSQ. J.D. has a Postdoctoral Fellowship from the Maisonneuve-Rosemont Research Centre. G.B. is supported by the Fonds de Recherche en Santé du Québec (FRSQ).

## References

Anthony, T.E., Klein, C., Fishell, G., Heintz, N., 2004. Radial glia serve as neuronal progenitors in all regions of the central nervous system. Neuron 41, 881–890.

Bernier, G., Panitz, F., Zhou, X., Hollemann, T., Gruss, P., Pieler, T., 2000. Expanded retina territory by midbrain transformation upon overexpression of *Six6* (*Optx2*) in *Xenopus* embryos. Mech. Dev. 93, 59–69.

Bernier, G., Vukovich, W., Neidhardt, L., Herrmann, B.G., Gruss, P., 2001. Isolation and characterization of a downstream target of *Pax6* in the mammalian retinal primordium. Development 138, 3987–3994.

Cartier, L., Laforge, T., Feki, A., Arnaudeau, S., Dubois-Dauphin, M., Krause, K.H., 2006. Pax6-induced alteration of cell fate: shape changes, expression of neuronal alpha tubulin, postmitotic phenotype, and cell migration. J. Neurobiol. 66, 421–436.

Chenn, A., Walsh, C.A., 2002. Regulation of cerebral cortical size by control of cell cycle exit in neural precursors. Science 297, 365–369.

Chow, R.L., Altmann, C.R., Lang, R.A., Hemmati-Brivanlou, A., 1999. Pax6 induces ectopic eyes in a vertebrate. Development 126, 4213–4222.

Collinson, J.M., Hill, R.E., West, J.D., 2000. Different roles for Pax6 in the optic vesicle and facial epithelium mediate early morphogenesis of the murine eye. Development 127, 945–956.

Del Bene, F., Tessmar-Raible, K., Wittbrodt, J., 2004. Direct interaction of geminin and Six3 in eye development. Nature 427, 745–749.

Duparc, R.H., Boutemmine, D., Champagne, M.P., Tétreault, N., Bernier, G., in press. Pax6 is required for *Delta-catenin/Neurojugin* expression during retinal, cerebellar and cortical development in mice. Dev. Biol. (Electronic publication ahead of print, August 9, 2006).

Dyer, M.A., Cepko, C.L., 2001. p27Kip1 and p57Kip2 regulate proliferation in distinct retinal progenitor cell populations. J. Neurosci. 21, 4259–4271.

Ellis, P., Fagan, B.M., Magness, S.T., Hutton, S., Taranova, O., Hayashi, S., McMahon, A., Rao, M., Pevny, L., 2004. SOX2, a persistent marker for multipotential neural stem cells derived from embryonic stem cells, the embryo or the adult. Dev. Neurosci. 26, 148–165.

Endl, E., Hollmann, C., Gerdes, J., 2001. Antibodies against the Ki-67 protein: assessment of the growth fraction and tools for cell cycle analysis. Methods Cell Biol. 63, 399–418.

Estivill-Torrus, G., Pearson, H., van Heyningen, V., Price, D.J., Rashbass, P., 2002. Pax6 is required to regulate the cell cycle and the rate of progression from symmetrical to asymmetrical division in mammalian cortical progenitors. Development 129, 455–466.

Fantes, J., Ragge, N.K., Lynch, S.A., McGill, N.I., Collin, J.R., Howard-Peebles, P.N., Hayward, C., Vivian, A.J., Williamson, K., van Heyningen, V., FitzPatrick, D.R., 2003. Mutations in SOX2 cause anophthalmia. Nat. Genet. 33, 461–463.

Fujiwara, M., Uchida, T., Osumi-Yamashita, N., Eto, K., 1994. Uchida rat (rSey): a new mutant rat with craniofacial abnormalities resembling those of the mouse Sey mutant. Differentiation 57, 31–38.

Gehring, W.J., 2002. The genetic control of eye development and its implications for the evolution of the various eye-types. Int. J. Dev. Biol. 46, 65–73.

Gehring, W.J., Kazuho, I., 1999. Pax6 mastering eye morphogenesis and eye evolution. Trends Genet. 15, 371–377.

Glaser, T., Jepea, l.L., Edwards, J.G., Young, S.R., Favor, J., Maas, R.L., 1994. PAX6 gene dosage effect in a family with congenital cataracts, aniridia, anophthalmia and central nervous system defects. Nat. Genet. 7, 463–471.

Gotz, M., Huttner, W.B., 2005. The cell biology of neurogenesis. Nat. Rev., Mol. Cell Biol. 6, 777–788.

Gotz, M., Stoykova, A., Gruss, P., 1998. Pax6 controls radial glia differentiation in the cerebral cortex. Neuron 21, 1031–1044.

Grindley, J.C., Davidson, D.R., Hill, R.E., 1995. The role of Pax-6 in eye and nasal development. Development 121, 1433–1442.

Halder, G., Callaerts, P., Gehring, W.J., 1995. Induction of ectopic eyes by targeted expression of the eyeless gene in *Drosophila*. Science 267, 1788–1792.

Haubst, N., Berger, J., Radjendirane, V., Graw, J., Favor, J., Saunders, G.F., Stoykova, A., Gotz, M., 2004. Molecular dissection of Pax6 function: the specific roles of the paired domain and homeodomain in brain development. Development 131, 6131–6140.

Heins, N., Malatesta, P., Ceccon, F., Nakafuku, M., Tucker, K.L., Hack, M.A., Chapouton, P., Barde, Y.A., Gotz, M., 2002. Glial cells generate neurons: the role of the transcription factor Pax6. Nat. Neurosci. 5, 308–315.

Hill, R.E., Favor, J., Hogan, B.L., Ton, C.C., Saunders, G.F., Hanson, I.M., Prosser, J., Jordan, T., Hastie, N.D., van Heyningen, V., 1991. Mouse small eye results from mutations in a paired-like homeobox-containing gene. Nature 354, 522–525.

Hock, H., Hamblen, M.J., Rooke, H.M., Schindler, J.W., Saleque, S., Fujiwara, Y., Orkin, S.H., 2004. Gfi-1 restricts proliferation and preserves functional integrity of haematopoietic stem cells. Nature 431, 1002–1007.

Hogan, B.L., Horsburgh, G., Cohen, J., Hetherington, C.M., Fisher, G., Lyon, M.F., 1986. Small eyes (Sey): a homozygous lethal mutation on chromosome 2 which affects the differentiation of both lens and nasal placodes in the mouse. J. Embryol. Exp. Morphol. 97, 95–110.

Huang, X., Wu, D.Y., Chen, G., Manji, H., Chen, D.F., 2003. Support of retinal ganglion cell survival and axon regeneration by lithium through a Bcl-2-dependent mechanism. Invest. Ophthalmol. Visual Sci. 44, 347–354.

Huttner, W.B., Kosodo, Y., 2005. Symmetric versus asymmetric cell division during neurogenesis in the developing vertebrate central nervous system. Curr. Opin. Cell Biol. 17, 648–657.

Hyer, J., 2004. Looking at an oft-overlooked part of the eye: a new perspective on ciliary body development in chick. Dev. Neurosci. 26, 456–465.

Jean, D., Bernier, G., Gruss, P., 1999. Six6 (Optx2) is a novel murine Six3-related homeobox gene that demarcates the presumptive pituitary/hypothalamic axis and the ventral optic stalk. Mech. Dev. 84, 31–40.

Kee, N., Sivalingam, S., Boonstra, R., Wojtowicz, J.M., 2002. The utility of Ki-67 and BrdU as proliferative markers of adult neurogenesis. J. Neurosci. Methods 115, 97–105.

Kippin, T.E., Martens, D.J., van der Kooy, D., 2005. p21 loss compromises the relative quiescence of forebrain stem cell proliferation leading to exhaustion of their proliferation capacity. Genes Dev. 19, 756–767.

Klezovitch, O., Fernandez, T.E., Tapscott, S.J., Vasioukhin, V., 2004. Loss of cell polarity causes severe brain dysplasia in Lgl1 knockout mice. Genes Dev. 18, 559–571.

Koso, H., Ouchi, Y., Tabata, Y., Aoki, Y., Satoh, S., Arai, K., Watanabe, S., 2006. SSEA-1 marks regionally restricted immature subpopulations of embryonic retinal progenitor cells that are regulated by the Wnt signaling pathway. Dev. Biol. 292, 265–276.

Krishan, A., 1975. Rapid flow cytofluorometric analysis of mammalian cell cycle by propidium iodide staining. J. Cell Biol. 66, 188–193.

Lee, A., Kessler, J.D., Read, T.A., Kaiser, C., Corbeil, D., Huttner, W.B., Johnson, J.E., Wechsler-Reya, R.J., 2005. Isolation of neural stem cells from the postnatal cerebellum. Nat. Neurosci. 8, 723–729.

Lien, W.H., Klezovitch, O., Fernandez, T.E., Delrow, J., Vasioukhin, V., 2006. alphaE-catenin controls cerebral cortical size by regulating the hedgehog signaling pathway. Science 311, 1609–1612.

Lillien, L., Raphael, H., 2000. BMP and FGF regulate the development of EGF-responsive neural progenitor cells. Development 127, 4993–5005.

Loosli, F., Winkler, S., Wittbrodt, J., 1999. Six3 overexpression initiates the formation of ectopic retina. Genes Dev. 13, 649–654.

Marquardt, T., 2003. Transcriptional control of neuronal diversification in the retina. Prog. Retinal Eye Res. 22, 567–577.

Marquardt, T., Ashery-Padan, R., Andrejewski, N., Scardigli, R., Guillemot, F., Gruss, P., 2001. Pax6 is required for the multipotent state of retinal progenitor cells. Cell 105, 43–55.

Mathers, P.H., Grinberg, A., Mahon, K.A., Jamrich, M., 1997. The Rx homeobox gene is essential for vertebrate eye development. Nature 387, 603–607.

Molofsky, A.V., Pardal, R., Iwashita, T., Park, I.K., Clarke, M.F., Morrison, S.J., 2003. Bmi-1 dependence distinguishes neural stem cell self-renewal from progenitor proliferation. Nature 425, 962–967.

Oliver, G., Gruss, P., 1997. Current views on eye development. Trends Neurosci. 20, 415–421.

Oliver, G., Mailhos, A., Wehr, R., Copeland, N.G., Jenkins, N.A., Gruss, P., 1995. Six3, a murine homologue of the sine oculis gene, demarcates the most anterior border of the developing neural plate and is expressed during eye development. Development 121, 4045–4055.

Philips, G.T., Stair, C.N., Young Lee, H., Wroblewski, E., Berberoglu, M.A., Brown, N.L., Mastick, G.S., 2005. Precocious retinal neurons: Pax6 controls timing of differentiation and determination of cell type. Dev. Biol. 279, 308–321.

Porter, F.D., Drago, J., Xu, Y., Cheema, S.S., Wassif, C., Huang, S.P., Lee, E., Grinberg, A., Massalas, J.S., Bodine, D., Alt, F., Westphal, H., 1997. Lhx2, a LIM homeobox gene, is required for eye, forebrain, and definitive erythrocyte development. Development 124, 2935–2944.

Quiring, R., Walldorf, U., Kloter, U., Gehring, W.J., 1994. Homology of the eyeless gene of *Drosophila* to the Small eye gene in mice and Aniridia in humans. Science 265, 785–789.

Scholzen, T., Gerdes, J., 2000. The Ki-67 protein: from the known and the unknown. J. Cell. Physiol. 182, 311–322.

St-Onge, L., Sosa-Pineda, B., Chowdhury, K., Mansouri, A., Gruss, P., 1997. Pax6 is required for differentiation of glucagon-producing alpha-cells in mouse pancreas. Nature 387, 406–409.

Temple, S., 2001. The development of neural stem cells. Nature 414, 112–117.

Tropepe, V., Sibilia, M., Ciruna, B.G., Rossant, J., Wagner, E.F., van der Kooy, D., 1999. Distinct neural stem cells proliferate in response to EGF and FGF in the developing mouse telencephalon. Dev. Biol. 208, 166–188.

Tropepe, V., Coles, B.L., Chiasson, B.J., Horsford, D.J., Elia, A.J., McInnes, R.R., van der Kooy, D., 2000. Retinal stem cells in the adult mammalian eye. Science 287, 2032–2036.

Turner, D.L., Cepko, C.L., 1987. A common progenitor for neurons and glia persists in rat retina late in development. Nature 328, 131–136.

Turner, D.L., Snyder, E.Y., Cepko, C.L., 1990. Lineage-independent determination of cell type in the embryonic mouse retina. Neuron 4, 833–845.

Viti, J., Feathers, A., Phillips, J., Lillien, L., 2003. Epidermal growth factor receptors control competence to interpret leukemia inhibitory factor as an astrocyte inducer in developing cortex. J. Neurosci. 23, 3385–3393.

Walther, C., Gruss, P., 1991. Pax-6, a murine paired box gene, is expressed in the developing CNS. Development 113, 1435–1449.

Yoon, K., Nery, S., Rutlin, M.L., Radtke, F., Fishell, G., Gaiano, N., 2004. Fibroblast growth factor receptor signaling promotes radial glial identity and interacts with Notch1 signaling in telencephalic progenitors. J. Neurosci. 24, 9497–9506.

Yu, X., Zhan, X., D'Costa, J., Tanavde, V.M., Ye, Z., Peng, T., Malehorn, M.T., Yang, X., Civin, C.I., Cheng, L., 2003. Lentiviral vectors with two independent internal promoters transfer high-level expression of multiple transgenes to human hematopoietic stem-progenitor cells. Mol. Ther. 7, 827–838.

Zhou, Y.H., Tan, F., Hess, K.R., Yung, W.K., 2003. The expression of PAX6, PTEN, vascular endothelial growth factor, and epidermal growth factor receptor in gliomas: relationship to tumor grade and survival. Clin. Cancer Res. 9, 3369–3375.

Zhou, Y.H., Wu, X., Tan, F., Shi, Y.X., Glass, T., Liu, T.J., Wathen, K., Hess, K.R., Gumin, J., Lang, F., Yung, W.K., 2005. PAX6 suppresses growth of human glioblastoma cells. J. Neuro-oncol. 71, 223–229.

Zimmerman, L., Parr, B., Lendahl, U., Cunningham, M., McKay, R., Gavin, B., Mann, J., Vassileva, G., McMahon, A., 1994. Independent regulatory elements in the nestin gene direct transgene expression to neural stem cells or muscle precursors. Neuron 12, 11–24.

Zuber, M.E., Perron, M., Philpott, A., Bang, A., Harris, W.A., 1999. Giant eyes in *Xenopus laevis* by overexpression of XOptx2. Cell 98, 341–352.